Molecular Crystals and Liquid Crystals

ISSN: 1542-1406 (Print) 1563-5287 (Online) Journal homepage: http://www.tandfonline.com/loi/gmcl20

Temporal Behavior of Photo-inscribed Grating in Azo-Carbazole Dyes Simultaneously Observed with Two-Beam Coupling in situ and Four-Wave Mixing

Kazuhiro Tada, Toshiro Imai & Yutaka Kawabe

To cite this article: Kazuhiro Tada, Toshiro Imai & Yutaka Kawabe (2015) Temporal Behavior of Photo-inscribed Grating in Azo-Carbazole Dyes Simultaneously Observed with Two-Beam Coupling in situ and Four-Wave Mixing, Molecular Crystals and Liquid Crystals, 621:1, 89-95, DOI: 10.1080/15421406.2015.1095966

To link to this article: http://dx.doi.org/10.1080/15421406.2015.1095966

Published online: 16 Dec 2015.

Mol. Cryst. Liq. Cryst., Vol. 621: pp. 89–95, 2015

ISSN: 1542-1406 print/1563-5287 online
DOI: 10.1080/15421406.2015.1095966

Taylor & Francis
Taylor & Francis Group

Temporal Behavior of Photo-inscribed Grating in Azo-Carbazole Dyes Simultaneously Observed with Two-Beam Coupling *in situ* and Four-Wave Mixing

KAZUHIRO TADA,* TOSHIRO IMAI, AND YUTAKA KAWABE

Chitose Institute of Science and Technology, Chitose, Hokkaido, Japan

An azo-carbazole dye has been known to show efficient dynamic holography characteristics. In order to investigate its mechanism, we made simultaneous measurements of two-beam coupling (TBC) in situ *and four-wave mixing (FWM) for the azo-carbazole dye, 3-[(4-Nitrophenyl)azo]-9H- carbazole-9-ethanol (NACzEtOH) doped in a polymer. The results showed fast temporal response with excitation at 532 nm, and slower rise and decay processes monitored at 785 nm. On the other hand, when excited at 633 nm only slow responses were observed. Simple analysis suggests that fast process was originated from photo-induced reorientation of the azo-carbazole dye and slower process was mainly caused by the following alignment of polymer matrix which played an important role for image preservation.*

Keywords organic photorefractive effect; refractive index grating; photo-isomerization; photo-isomerization; photo-orientation; azo-carbazole

1. Introduction

Azo-carbazole dyes are considered to be promising candidates for dynamic three-dimensional displays of next generation because of their high holographic performance. Azo-carbazoles such as 3-[(4-Nitrophenyl)- azo]-9H-carbazole-9-ethanol (NACzEtOH) heavily doped in poly(methyl methacrylate) (PMMA) were employed as a medium for holography, giving fast response to optical writing and long persistency of memorized images [1, 2]. Because several mechanisms as photo-isomerization and photo-alignment of dyes, and induced polymer alignment would contribute to the process, precise measurements at multiple wavelengths will give insights into their details.

We have studied the photo-induced grating in NACzEtOH mainly with two methods. One technique was two-beam coupling (TBC) or its variation so called TBC *in situ* in which writing and reading were made by the same wavelength [3–5]. With this technique several groups including us reported a strange energy transfer in matrices heavily containing azo chromophores even under no external electric field and nominally fully symmetric optical alignments [6–11]. The other method was non-degenerate four-wave mixing (FWM) using

*Address correspondence to Kazuhiro Tada, Chitose Institute of Science and Technology, 758-65 Bibi, Chitose, Hokkaido 066-8655, Japan. E-mail: k-tada@photon.chitose.ac.jp

Color versions of one or more of the figures in the article can be found online at www.tandfonline.com/gmcl.

different wavelength source for the writing and reading, of which optical setup was basically the same as holography [4, 12–14].

With TBC, one can mainly observe the behavior of dopant dyes according to the wavelength resonant to the absorption band of dye. On the other hand, effects from polymer matrix would not be negligible in FWM, because the media is usually transparent at the probe wavelength. Our preceding studies have shown the temporal behavior of refractive index modulation and phase displacement of photo-induced grating. The results gave slow response in TBC at 633 nm (almost transparent) with a thick sample, and relatively fast inscription at 532 nm (absorbing) monitored with the FWM alignment for thin films [4, 5].

In this study, we combined the two methods in order to observe the behavior simultaneously at two wavelengths giving complimentary information. Absorption edge of NACzEtOH (30 wt%) in PMMA was located at around 600 nm, but there was a residual tail up to longer wavelength side. Therefore, lasers of 532 and 633 nm were used as excitation sources (which also works as probes in TBC), and 785 nm laser was employed for probing in FWM measurements.

2. Experimental

NACzEtOH doped in PMMA films with 30 wt% concentration were employed as samples. Films were prepared with a spin-coating method in which the thickness was adjusted to be about 4 μm. The chemical structure of the compound is shown in Fig. 1 (a). The absorption spectrum in Fig 1 (b) indicates that the optical density of the sample at 532 and 633 nm are 1.29 and 0.00147, respectively.

The experimental setup is depicted in Fig. 2. The apparatus was composed of a simple symmetric two-beam interferometer and a probe laser. A laser beam for TBC was divided into two parts by a beam splitter, then being directed into a sample for interference. For the TBC experiment, two types of exciting lasers were incorporated, that is, a He-Ne laser (Spectra-Physics, model 127) operating at the wavelength of 633 nm and a diode-pumped solid-state laser (Coherent, COMPASS532-50-YS) at 532 nm. For FWM alignment, a diode laser (Thorlabs, LPS-PM785-FC) of 785 nm was used as a reading beam. The polarization of both exciting lasers was set to be p directions with a Glan-Thompson prism and a half-wavelength plate. The 785 nm probe laser was also set to be p-polarized. Intensities

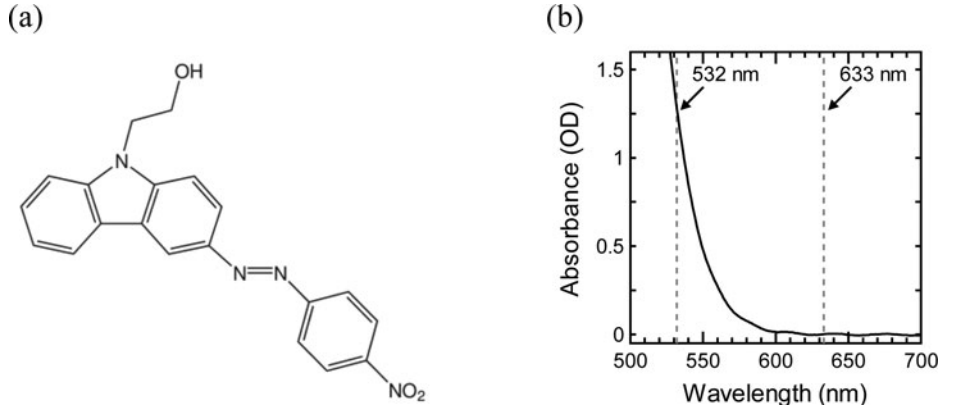

Figure 1. (a) The structural formula of NACzEtOH. (b) Absorption spectrum of a spin-coated NACzEtOH/PMMA films with 4-μm-thickness.

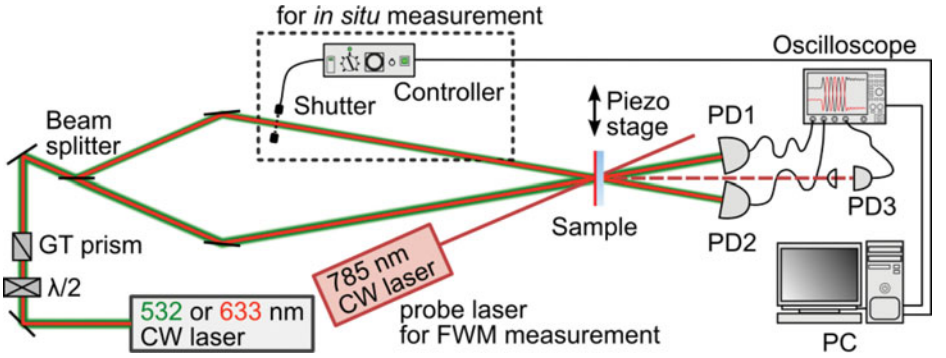

Figure 2. Experimental setup of TBC *in situ* and FWM measurements. Here, λ/2: half-wave plate, GT prism: Glan-Thompson prism, PD: photodetector.

of the transmitted pump beams were monitored by two photo-detectors (PD1 and PD2), and the third detector PD3 was used for monitoring of the FWM diffraction intensity. The incident laser power and diameter were 0.4 mW and 1 mm, respectively, for both beams. The crossing angle of the incident beams was 11.2 degree, and the sample was set normal to the bisector of the two incident beams.

The measurement was composed of two steps. At first, grating formation (writing) was made for about 1000 sec by excitation beams. During the writing, diffraction at 785 nm was monitored continuously, while the mechanical shutter was closed for 0.5 sec in every 10 sec in order to determine diffraction intensity observed at the writing wavelength. In the second step, erasure process of the grating was monitored at two wavelengths under the illumination of one excitation beam for about 1000 sec.

3. Results

3.1. Dynamics with 532 nm Laser Writing

Typical traces for TBC *in situ* (532 nm writing) and FWM (785 nm probe) measurements are shown in Fig. 3. Here, 'TBC signal' drawn by thin black curve is the intensity monitored with PD1. 'TBC *in situ*' indicates the intensity at PD2 giving dips when the shutter was closed. The vertical scale is expanded to show the dip positions indicating the diffraction intensity when only one beam was incident. On the other hand, 'FWM' curve gives the growth of the grating observed at the near IR wavelength.

Normalized diffraction intensity of both signals during rise and erasure are shown in Fig. 4 (a) and (b). The diffraction for the *in situ* measurement showed relatively strong instantaneous response, then reduced to a minimum value about after 200 sec to get increase again. On the other hand, the result of FWM measurement gave gradual increase and saturation of diffraction intensity after around 800 sec. Therefore, different types of growing mechanisms must have contributed to each grating sensitive to visible and near IR light.

Indeed, different behaviors were also observed in erasure process as shown in Fig. 4 (b), that is, apparently fast and marginal components were observed in the decay of TBC signal, while only slow decay seemed to appear in FWM process.

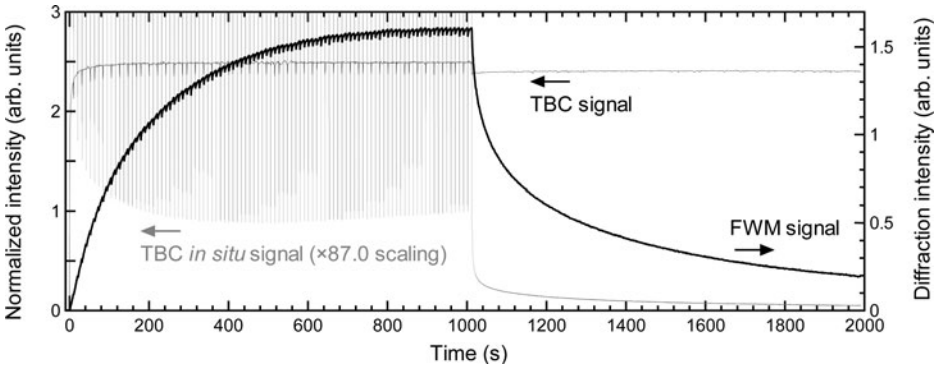

Figure 3. Results of TBC *in situ* (532 nm writing) and FWM (785 nm probe) measurement. Thin black curve, gray curve, and bold black curve show TBC signal (PD1), TBC *in situ* signal (PD2), and FWM signal (PD3), respectively. Intensity of PD1 is normalized by the initial ($t = 0$) value.

TBC signal indicated by the thin curve in Fig. 3 showed that the transmitted light intensities became about 2.5 times larger than the initial value immediately after the start of irradiation. Such a fast response was likely due to photo-orientation effect following *trans-cis* photo-isomerization induced by the light absorption in the main band of the compound, reflecting the efficiency of molecular motion. The change of the extinction coefficient $\Delta\kappa$ was estimated to be 0.00075 after laser irradiation. After turning one beam off, the value only reduced to 0.00072, indicating the saturation of molecular orientation under the excitation of several ten mW/cm^2.

3.2. Dynamics with 633 nm Laser Writing

Even though the absorption coefficient at 633 nm was much smaller than that at 532 nm, grating inscription and its phase displacement have been observed in TBC made at this wavelength [4, 5]. Total absorption of the sample at 633 nm was about 0.3%. Fig. 5 shows the traces of TBC *in situ* (633 nm writing) and FWM (785 nm probe) observed simultaneously. As Fig. 3, thin black curve, gray curve, and thick black curve show TBC

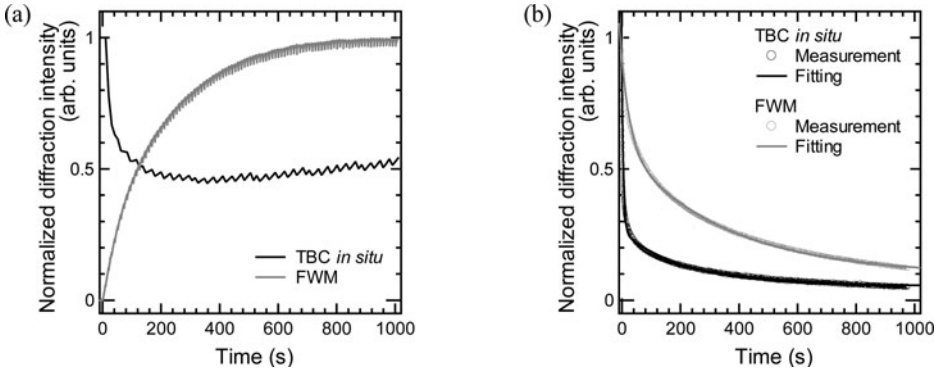

Figure 4. (a) and (b) show rise and erase process of normalized diffraction intensity of TBC (532 nm) and FWM (785 nm). The fitting parameters of (b) see Table I.

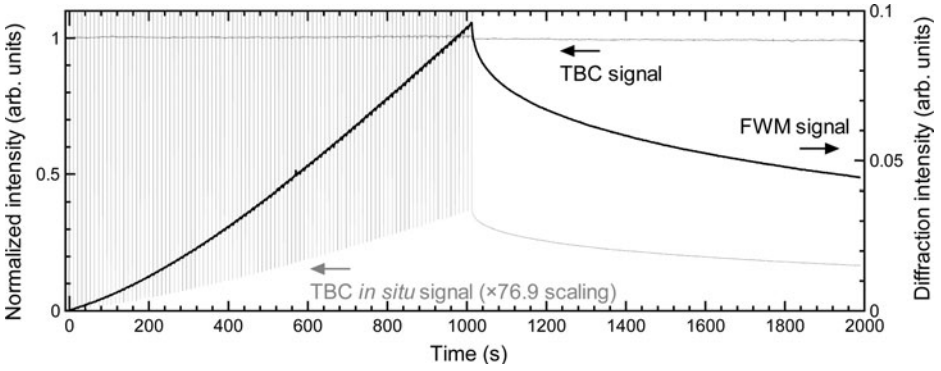

Figure 5. Results of TBC *in situ* (633 nm writing and probing) and FWM (785 nm probing) measurements. Thin black curve, gray curve, and thick black curve show TBC signal, TBC *in situ* signal, and FWM signal, respectively.

signal (PD1), TBC *in situ* signal (PD2), and FWM signal (PD3), respectively. Contrary to the case of the former results, the diffraction intensities increased monotonically for both wavelengths and decayed also in a similar way. Both processes are shown in Fig. 6 (a) and (b) with normalized scales. Because there must be no absorption in near IR region, the correspondence shows that the diffraction was caused by refractive index change with the same origin at these two wavelengths.

4. Discussion and Conclusion

We made fitting of the decay curves in order to investigate the erasing process under laser illumination at two wavelengths. The decaying curves were known to consist of more than two temporal components. Therefore, we analyzed the behavior with bi-exponential fitting. The curves are assumed to be given as the function of time t by $I = C_0 + C_1\exp(-t/\tau_1) + C_2\exp(-t/\tau_2)$, where C, τ are constants for magnitudes and time constants, respectively. The parameters obtained by the fittings are given in Table I. Estimated time constants can be classified into three types of values. Among them, the fastest response was only observed in

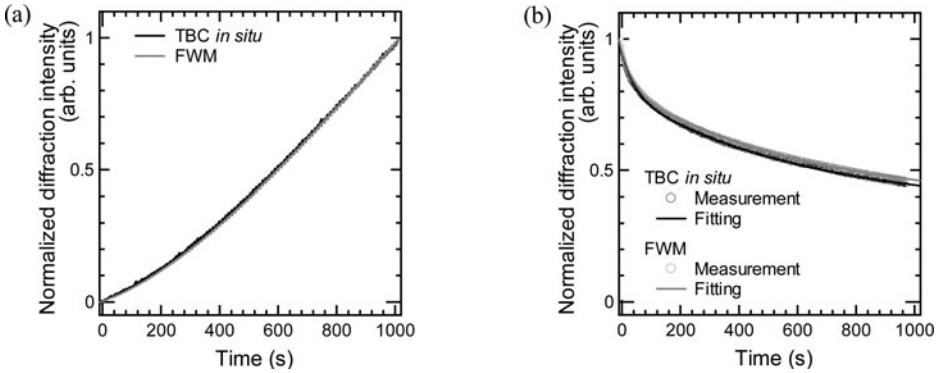

Figure 6. (a) and (b) show rise and erase processes of normalized diffraction intensity of TBC (633 nm) and FWM (785 nm). For fitting parameters of (b), see Table I.

Table 1. The fitting parameters of the erasing process (Fig. 4 (b) and Fig. 6 (b)).

	Reading	C_0	C_1	τ_1 (sec)	C_2	τ_2 (sec)
633 nm writing	633 nm TBC	0.36	0.15	45	0.44	620
	785 nm FWM	0.37	0.15	44	0.44	630
532 nm writing	532 nm TBC	0.055	0.55	5.5	0.21	220
	785 nm FWM	0.097	0.34	31	0.48	350

TBC experiment with 532 nm. Because the response probed at 532 nm might be dominated by the main absorption band of the dye, the modulation of optical constant observed in this region would be determined by the motion of the dye. Therefore, the fastest component should reflect the optical alignment and following orientation relaxation processes.

Two constants appeared in 633 nm writing experiments should be assigned to identical origin, since all parameters at two wavelengths were the same. However, main contribution was not made by the dye alignment, because temporal evolution differed from the case for 532 nm. Considering that there seemed no effects from dispersion at 633 and 785 nm, it is reasonable to attribute the origin to the birefringence induced in polymer matrix. Values of Δn just before the decay were estimated to be 0.00353 at 633 nm.

The result of FWM by 532 nm excitation could also be attributed to the polymer matrix. However, the effects from dye orientation could not be negligible in this case, and that would be the reason why time constant values deviated from those observed in 633 nm excitation. In this context, strange behavior observed in the growing process of TBC at 532 nm can be considered to be superposition of fast response by the dye and slow polymer response with the opposite sign, although the slight increase after 400 sec cannot be explained well. In order to distinguish the contributions from dye and polymer more precisely, supplemental experiments including long time measurement, concentration dependence and likes will be required. Some of them are in progress, now.

Even though the absorption coefficient at 633 nm was quite weak, grating inscription must have started with light absorption by the dye. In this case, although the number of molecules experiencing the photo-alignment was small leading to weak response, they could accumulate the effects of the polymer reorientation as assumed by the growth trace given in Fig. 6 (a), and the origin of the grating made will be attributed to refractive index change only in the polymer.

In conclusion, we demonstrated simultaneous measurements of TBC *in situ* and FWM for azo-carbazole dye, NACzEtOH with excitation at 532 and 633 nm and reading at 785 nm. Simple analyses for the temporal evolution of the photo-induced grating formation and erasure processes showed that 532 nm excitation induced relatively fast response of the dye followed by slower evolution occurred in the polymer matrix. This conjecture can explain the fast response and long persistency achieved in the dynamic holography with NACzEtOH [1, 2]. And the results also strongly suggest that the strange symmetry-braking observed NACzEtOH under the 633 nm excitation relates to polymer motion [3–5]. These characteristics are important for practical applications, so further studies would be required to optimize the material parameters.

Acknowledgments

This work was partially supported by “Program for Strategic Promotion of Innovative Research and Development” from JST, Japan. A part of this work was supported by

Nanotechnology Platform Program (Synthesis of Molecules and Materials) of the Ministry of Education, Culture, Sports, Science and Technology (MEXT), Japan.

References

[1] Tsutsumi, N., Kinashi, K., Sakai, W., Nishide, J., Kawabe, Y., & Sasabe, H. (2012). *Opt. Mater. Express*, *2*, 1003–1010.
[2] Tsutsumi, N., Kinashi, K., Tada, K., Fukuzawa, K., & Kawabe, Y. (2013). *Opt. Express*, *21*, 19880–19884.
[3] Nishide, J., Tanaka, A., Hirama, Y., & Sasabe, H. (2008). *Mol. Cryst. Liq. Cryst.*, *491*, 217–222.
[4] Kawabe, Y., Fukuzawa, K., Uemura, T., Matsuura, K., Yoshikawa, T., Nishide, J., & Sasabe, H. (2012). *Appl. Opt.*, *51*, 6653–6660.
[5] Tada, K., Fukuzawa, K., Yoshikawa, T., Imai, T., & Kawabe, Y. (2015). *Nonlin. Opt. Quant. Opt., 47,* 59–71.
[6] Zhang, W., Bian, S., Kim, S. I., & Kuzyk, M. G. (2002). *Opt. Lett.*, *27*, 1105–1107.
[7] Bian, S. & Kuzyk, M. G. (2002). *Opt. Lett.*, *27*, 1761–1763.
[8] Cheben, P., del Monte, F., Worsfold, D. J., Carlsson, D. J., Grover, C. P., & Mackenzie, J. D. (2000). *Nature*, *408*, 64–67.
[9] Lee, J.-W., Mun, J., Yoon, C. S., Lee, K.-S., & Park, J.-K. (2002). *Adv. Mater.*, *14*, 144–147.
[10] Tsutsumi, N. & Shimizu, Y. (2004). *Jpn. J. Appl. Phys.*, *43*, 3466–3472.
[11] Gallego-Gomez, F., Del Monte, F., & Meerholz, K. (2008). *Nature Mater.*, *7*, 490–497.
[12] Zhao, Y. & Ikeda, T. eds. (2009) *Smart light-responsive matters*, Wiley, Hoboken.
[13] Barrett, C. J., Natansohn, A. L., & Rochon, P. L. (1996). *J. Phys. Chem.*, *100*, 8836–8842.
[14] Blanche, P.-A., Lamaire, Ph. C., Maertens, C., Dubois, P., & Jérôme, R. (2000). *J. Opt. Soc. Am. B*, *17*, 729–740.